ORGANOMETALLICS
Article

Organometallics **2010,** *29,* 2413–2421 2413
DOI: 10.1021/om901028z

Phosphinoureas: Cooperative Ligands in Rhodium-Catalyzed Hydroformylation? On the Possibility of a Ligand-Assisted Reductive Elimination of the Aldehyde

Jurjen Meeuwissen,[†] Albertus J. Sandee,[†,‡] Bas de Bruin,[†] Maxime A. Siegler,[§] Anthony L. Spek,[§] and Joost N. H. Reek*[,†]

[†]*Van't Hoff Institute for Molecular Sciences, University of Amsterdam, Nieuwe Achtergracht 166, 1018 WV Amsterdam, The Netherlands,* [‡]*BASF Nederland B.V. Catalysts, Strijkviertel 67, 3454 PK De Meern, The Netherlands, and* [§]*Crystal and Structural Chemistry, Bijvoet Centre for Biomolecular Research, Faculty of Science, Utrecht University, Padualaan 8, 3584 CH Utrecht, The Netherlands*

Received November 27, 2009

We report the synthesis of a novel type of phosphinourea ligand, its coordination chemistry with rhodium, its use in the asymmetric hydroformylation of styrene, and investigations on the hydroformylation reaction mechanism. Complex studies on the 2:1 complex of phosphinourea to [Rh(acac)-$(CO)_2$] showed that a neutral *trans*-coordinating complex [Rh(*H*L-κP)(L-$\kappa^2 O,P$)(CO)] was formed. An anionic *O*,*P*-chelating ligand has displaced the anionic acac$^-$ ligand via an acid−base reaction involving the deprotonation of an acidic urea proton, giving *H*acac. A second phosphinourea is coordinated as a neutral monodentate ligand and is linked to the chelating anionic ligand via an intramolecular hydrogen bond. The behavior of these supramolecular complexes in the hydroformylation reaction and the possible cooperative role of the ligands in the catalytic cycle were studied both experimentally and by computational methods. High-pressure NMR spectroscopy revealed that the catalytically active rhodium hydride species further consists of two neutral phosphinourea ligands and is in equilibrium with the neutral species [Rh(*H*L-κP)(L-$\kappa^2 O,P$)(CO)]. This equilibrium is likely an integrated part of a productive hydroformylation cycle involving a ligand-assisted reductive elimination of the aldehyde. DFT calculations revealed that the ligand-assisted mechanism could well be the preferred lower energetic pathway; however, the orientation of the anionic oxygen donor atom in [Rh(*H*L-κP)(L-$\kappa^2 O,P$)(CO)] prevented us from finding a direct (nonsolvent assisted) transition state to connect the intermediates. We therefore cannot exclude a mechanism where [Rh(*H*L-κP)(L-$\kappa^2 O,P$)-(CO)] is a dormant species outside the productive hydroformylation cycle, although the intermediate associated with this mechanism is higher in energy. Finally, the synthesis of heteroligated complexes was investigated, consisting of two electronically different phosphinoureas, which sets the stage for combinatorial supramolecular ligand approaches in catalysis. Simply mixing two electronically different phosphinoureas with metal precursor [Rh(acac)$(CO)_2$] resulted in the formation of a heterobidentate ligand. A set of six new phosphinoureas was used to prepare such rhodium complexes in a combinatorial fashion for the asymmetric hydroformylation of styrene, resulting in high conversions and selectivities for the branched product and moderate enantioselectivities.

Introduction

Traditionally, "catalysis by ligand design" means that variation of the steric and electronic properties of ligands is used to influence the catalytic performance of a catalyst as a whole. More recently, new developments invoke a more active role of the ligands, in which they are considered as an integrated part of the catalyst, strongly partaking in the reaction mechanism. Among such integrated catalysts are ligands capable of substrate orientation,[1] hemilabile (hybrid) ligands,[2] cooperative ligands,[3,4] or a combination these functionalities. Ligands with functionality for substrate orientation preorganize the substrate in a favorable way to

*To whom correspondence should be addressed. E-mail: j.n.h.reek@uva.nl. Fax: +31 (0)20 525 6422. Tel: +31 (0)20 525 6437.

(1) (a) Breuil, P.-A. R.; Patureau, F. W.; Reek, J. N. H. *Angew. Chem., Int. Ed.* **2009**, *48*, 2162–2165. (b) Šmejkal, T.; Breit, B. *Angew. Chem., Int. Ed.* **2008**, *47*, 311–315. (c) Šmejkal, T.; Breit, B. *Angew. Chem., Int. Ed.* **2008**, *47*, 3946–3949. (d) Grünanger, C. U.; Breit, B. *Angew. Chem., Int. Ed.* **2008**, *47*, 7346–7349. (e) Börner, A. *Chirality* **2001**, *13*, 625–628. (f) Börner, A. *Eur. J. Inorg. Chem.* **2001**, 327–337. (g) Sawamura, M.; Ito, Y. *Chem. Rev.* **1992**, *92*, 857–871.

(2) (a) Braunstein, P. *J. Organomet. Chem.* **2004**, *689*, 3953–3967. (b) Braunstein, P.; Naud, F. *Angew. Chem., Int. Ed.* **2001**, *40*, 680–699.

(3) Grützmacher, H. *Angew. Chem., Int. Ed.* **2008**, *47*, 1814–1818.

(4) (a) Patureau, F. W.; Kuil, M.; Sandee, A. J.; Reek, J. N. H. *Angew. Chem., Int. Ed.* **2008**, *47*, 3180–3183. (b) Gunanathan, C.; Ben-David, Y.; Milstein, D. *Science* **2007**, *317*, 790–792. (c) Zweifel, T.; Naubron, J.-V.; Grützmacher, H. *Angew. Chem., Int. Ed.* **2009**, *48*, 559–563. (d) Maire, P.; Böttner, T.; Breher, F.; Le Floch, P.; Grützmacher, H. *Angew. Chem., Int. Ed.* **2005**, *44*, 6318–6323. (e) Noyori, R.; Yamakawa, M.; Hashiguchi, S. *J. Org. Chem.* **2001**, *66*, 7931–7944.

Published on Web 05/13/2010

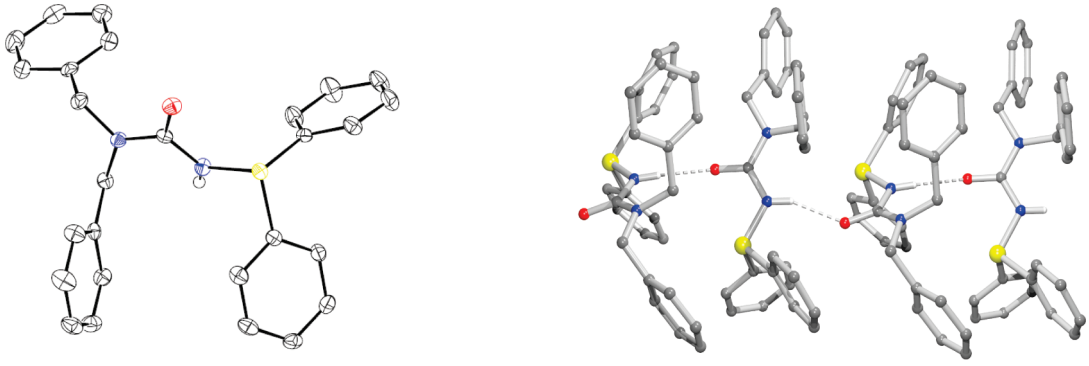

Figure 1. (Left) Displacement ellipsoid plot (50% probability level) of one of the two crystallographically independent molecules of ***H*L1** (CH hydrogen atoms omitted for clarity). The molecules link into infinite chains through NH···O hydrogen bonds. (Right) POV-Ray picture showing the 1D chain built of molecules of ***H*L1** via N−H···O hydrogen bond interactions (2.109 and 2.177 Å). P: yellow, O: red, N: blue, C: black, H: white.

enhance selectivity and activity. Breit and Reek exploited hydrogen bonding as a tool for substrate orientation. This strategy was demonstrated to be effective for the highly selective hydroformylation of unsaturated carboxylic acids with guanidinium-functionalized phosphines[1b,c] and for the hydrogenation of 2-hydroxymethylacrylate using a supramolecular heterobidentate ligand[5] of LEUPhos[1a] and a urea-functionalized phosphine. In these examples hydrogen bonding between the substrate and the ligand plays a crucial role to obtain high selectivity. Hemilabile ligands generally consist of a strongly coordinating donor atom and an additional weakly coordinating donor atom that can temporarily coordinate to the transition metal to stabilize reactive intermediates. Cooperative ligands were recently defined by Grützmacher[3] as ligands that participate directly in a bond activation reaction and undergo reversible chemical transformations. Milstein combined hemilabile and cooperative functionalities in a Ru^{II} complex based on a 2-(di-*tert*-butylphosphinomethyl)-6-(diethylaminomethyl)pyridine "pincer" ligand for the unprecedented dehydrogenative coupling of alcohols and amines to yield amides.[4c] The reversible ligand-assisted heterolytic splitting of H_2 was observed to be a key step in the mechanism. These examples clearly demonstrate that the role of the ligand in transition metal catalysis may be far less static than originally anticipated. In this paper we report on a new type of phosphinourea ligand that forms heterobidentate rhodium complexes via self-assembly. The experimental and computational studies point at a ligand-assisted (cooperative) mechanism in hydroformylation, implying an active role of this particular ligand in this reaction. Interestingly, the approach can be extended to supramolecular heterobidentate ligands, which sets the stage for combinatorial approaches. This is demonstrated by the preparation of 14 complexes using combinations of phosphinourea ligands and their application in the asymmetric hydroformylation reaction.

Results and Discussion

The general procedure for the preparation of phosphinourea ligands described in this paper consists of two steps: (1) the conversion of a secondary amine into a *N*,*N*-disubstituted urea, followed by (2) a condensation reaction of the *N*,*N*-disubstituted urea with a PCl compound.[6,7] These ligands all contain a phosphorus donor atom directly connected to a urea motif. For example, phosphorus amide ***H*L1** was prepared by converting *N*,*N*-dibenzyl urea into a lithium salt, which was subsequently reacted with chlorodiphenylphosphine (Scheme 1). The X-ray structure of ***H*L1** shows that in the solid state the molecules are linked through hydrogen bonding via the urea motif (Figure 1).

Scheme 1. Synthesis of Phosphinourea Ligand *H*L1

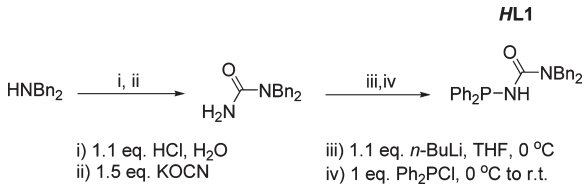

Addition of two equivalents of ***H*L1** to a solution of $[Rh(acac)(CO)_2]$ in $CDCl_3$ resulted in the formation of a yellow solution of complex [Rh(***H*L1**-κP)(**L1**-$\kappa^2 O,P$)(CO)] (Scheme 2, I).[4a,8] Two doublets of doublets resonating at δ 62.9 ppm ($^1J_{P-Rh}$ = 135 Hz) and at δ 82.0 ppm ($^1J_{P-Rh}$ = 129 Hz) are visible in the $^{31}P\{^1H\}$ NMR spectrum. The large P−P coupling constant ($^2J_{P-P}$ = 326 Hz) indicates that two inequivalent phosphorus ligands are in mutual *trans*-positions (Scheme 2, II). The ^1H NMR spectrum shows free acetylacetone (*H*acac) displaced from the metal complex and that one urea proton has disappeared. This implies that the acidic urea proton has been transferred to $acac^-$, yielding *H*acac and an anionic ligand $\mathbf{L1}^-$, which presumably coordinates in a bidentate fashion ($\kappa^2 P,O$), forming a five-membered ring.[9]

(5) (a) Wilkinson, M. J.; van Leeuwen, P. W. N. M.; Reek, J. N. H. *Org. Biomol. Chem.* **2005**, *3*, 2371–2383. (b) Breit, B. *Angew. Chem., Int. Ed.* **2005**, *44*, 6816–6825. (c) Sandee, A. J.; Reek, J. N. H. *Dalton Trans.* **2006**, 3385–3391.

(6) A similar phosphinourea ligand was reported before; see: Marchenko, A. P.; Koydan, G. K.; Smaliy, R. V.; Chaykovskaya, A. A.; Pinchuk, A. M.; Tolmachev, A. A.; Shishkin, O. V. *Eur. J. Inorg. Chem.* **2008**, 3348–3352.

(7) For reports on related compounds see: (a) Kühl, O.; Lönnecke, P. *Inorg. Chem.* **2002**, *41*, 4315–4317. (b) Kühl, O. *Dalton Trans.* **2003**, 949–952. (c) Kühl, O. *Coord. Chem. Rev.* **2006**, *250*, 2867–2915. (d) Bhattacharyya, P.; Slawin, A. M. Z.; Smith, M. B.; Williams, D. J.; Woollins, J. D. *J. Chem. Soc., Dalton Trans.* **1996**, 3647–3651. (e) Slawin, A. M. Z.; Wainwright, M.; Woollins, J. D. *J. Chem. Soc., Dalton Trans.* **2001**, 2724–2730.

(8) For similar metal complexes see: (a) Fuentes, J. A.; Clarke, M. L.; Slawin., A. M. Z. *New J. Chem.* **2008**, *32*, 689–693. (b) Trzeciak, A. M.; Štěpnička, P.; Mieczyńska, A. E.; Ziółkowski, J. J. *J. Organomet. Chem.* **2005**, *690*, 3260–3267. (c) Trzeciak, A. M.; Ziółkowski, J. J.; Tadeusz, L.; Choukroun, R. *J. Organomet. Chem.* **1999**, *575*, 87–97.

(9) A related anionic phosphinoamide ligand has been found to coordinate to rhodium via a *O*,*P* chelate; see: Braunstein, P.; Heaton, B. T.; Jacob, C.; Manzi, L.; Morise, X. *Dalton Trans.* **2003**, 1396–1401.

Scheme 2. (I) Reactivity of *H*L1 with [Rh(acac)(CO)$_2$]; (II) ^{31}P{^{1}H} NMR spectrum of the resulting complex [Rh(*H*L1-κ*P*)(L1-κ^2*O*,*P*)(CO)] (20 mM in $CDCl_3$)

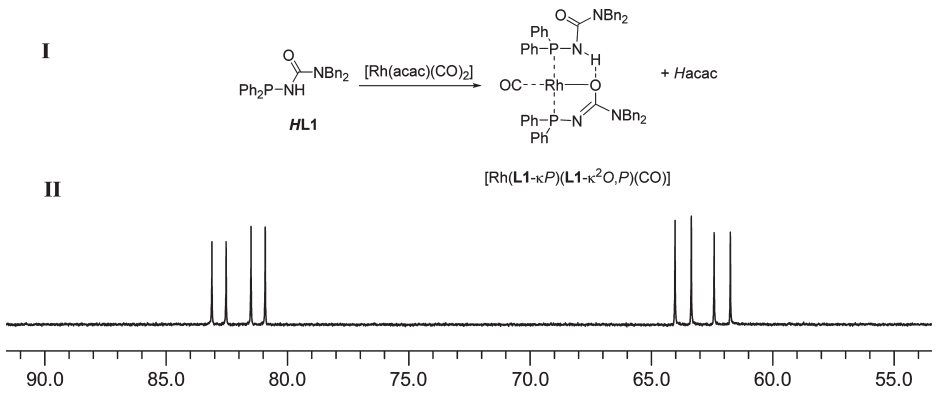

Additional proof for the urea proton abstraction from one of the ligands was obtained by proton-coupled ^{31}P NMR spectroscopy, showing that the signal resonating at δ 62.9 ppm has retained the P−H coupling ($^2J_{P-H}$ = 14.6 Hz, P with the urea proton) and thus corresponds to the neutral ligand. The signal resonating at δ 82.0 ppm lacks this coupling and thus corresponds to the (deprotonated) anionic ligand.[10] The ^{31}P{^{1}H}−^{1}H 2D-NMR spectrum shows that the single urea proton in the ^{1}H NMR correlates to the signal resonating at δ 62.9 ppm in the ^{31}P{^{1}H} NMR spectrum, providing further evidence that this peak corresponds to the neutral ligand.[10]

The urea proton signal in the ^{1}H NMR spectrum of the neutral ligand in the complex has shifted downfield by ~1.4 ppm compared to the free ligand, indicating that this proton is involved in hydrogen bonding, presumably via the coordinating oxygen atom of the anionic ligand (Scheme 2).[11] The proposed geometry of [Rh(***H*L1**-κ*P*)(**L1**-κ^2*O*,*P*)(CO)] in Scheme 2, I, is supported by the DFT-optimized structure (benzyl groups simplified to methyl groups), showing the two P atoms of the chelating anionic ligand and the neutral ligand in a *trans*-geometry (Figure 2).[12,14] The anionic (π-donating) oxygen donor and the π-accepting CO ligand coordinate preferably in mutual *trans*-positions for electronic reasons.[13] The DFT-optimized structure further reveals a NH···O distance of 1.973 Å, indicative of hydrogen bonding.[14] The complex was further characterized by solution IR spectroscopy, showing the coordinated CO ligand (ν(CO) = 1970 cm^{-1}), and mass spectrometry (*m*/*z* calcd for $C_{54}H_{49}N_4O_2P_2Rh$ 950.2386, found 950.2380 (CO ligand dissociated)).

We subsequently investigated the activity of [Rh(***H*L1**-κ*P*)-(**L1**-κ^2*O*,*P*)(CO)] in the hydroformylation of styrene, while varying several reaction parameters, such as the rhodium concentration and the partial pressures of CO and H_2 (Table 1). The complex is indeed an active catalyst and showed in all cases good selectivity for the branched product (95.3−96.2%). Because it is generally believed that a hydride species is the actual catalytically active species in hydroformylation, we initially considered [Rh(***H*L1**-κ*P*)(**L1**-κ^2*O*,*P*)(CO)] merely as a precursor complex for a hydride-containing

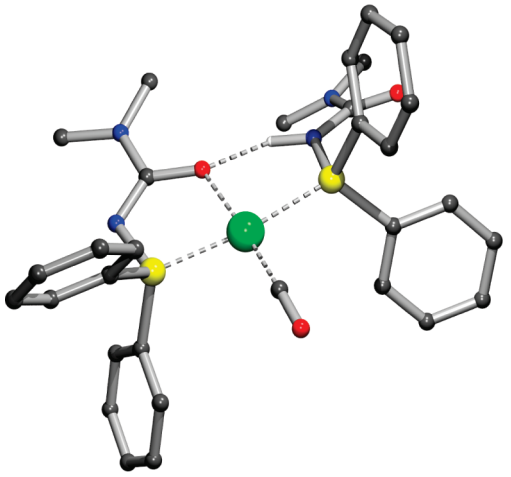

Figure 2. DFT (BP86, SV(P))-optimized structure of [Rh(*H*L-κ*P*)(L-κ^2*O*,*P*)(CO)], *H*L = 1,1-dimethyl-3-(diphenylphosphino)-urea (Rh−CO 1.818 Å, Rh−P(κ*P*) 2.349 Å, Rh−P(κ^2*O*,*P*) 2.317 Å, Rh−O 2.115 Å, O···HN 1.973 Å). CH hydrogen atoms are omitted for clarity. Rh: green, P: yellow, O: red, N: blue, C: black, H: white.

Table 1. Hydroformylation of Styrene Using [Rh(*H*L1-κ*P*)-(L1-κ^2*O*,*P*)(CO)][a]

entry	Rh [mM]	*p*CO (bar)	*p*H$_2$ (bar)	conversion (%)	branched (%)
1	1	10	10	6.2	95.8
2	5	10	10	26.5	95.3
3	10	10	10	32.3	95.4
4	15	10	10	33.2	95.3
5	5	10	30	62.0	95.4
6	5	30	10	18.7	96.2
7	5	20	20	22.2	96.0

[a] Reaction conditions: Rh = [Rh(acac)(CO)$_2$], [***H*L1**] = 2.1 × [Rh], [S] = 1 M, S = styrene, reaction time = 6 h, temperature = 40 °C, solvent = CH_2Cl_2.

(10) See Supporting Information.

(11) For other examples of supramolecular urea-functionalized ligands see: (a) Meeuwissen, J.; Kuil, M.; van der Burg, A. M.; Sandee, A. J.; Reek, J. N. H. *Chem.—Eur. J.* **2009**, *15*, 10272–10279. (b) Sandee, A. J.; van der Burg, A. M.; Reek, J. N. H. *Chem. Commun.* **2007**, 864–866. (c) Knight, L. K.; Freixa, Z.; van Leeuwen, P. W. N. M.; Reek, J. N. H. *Organometallics* **2006**, *25*, 954–960. (d) Duckmanton, P. A.; Blake, A. J.; Love, J. B. *Inorg. Chem.* **2005**, *44*, 7708–7710. (e) Yoo, H.; Mirkin, C. A.; DiPasquale, A. G.; Rheingold, A. L.; Stern, C. L. *Inorg. Chem.* **2008**, *47*, 9727–9729.

(12) We have attempted several times to crystallize [Rh(***H*L1**-κ*P*)-(**L1**-κ^2*O*,*P*)(CO)]; however we were not able to obtain crystals suitable for X-ray analysis.

(13) (a) Tejel, C.; Ciriano, M. A.; del Río, M. P.; Hetterscheid, D. G. H.; Tsichlis i Spithas, N.; Smits, J. M. M.; de Bruin, B. *Chem.—Eur. J.* **2008**, *14*, 10932–10936. (b) Tejel, C.; del Río, M. P.; Ciriano, M. A.; Reijerse, E. J.; Hartl, F.; Záliš, A.; Hetterscheid, D. G. H.; Tsichlis i Spithas; de Bruin, B. *Chem.—Eur. J.* **2009**, *15*, 11878–11889.

(14) The corresponding anionic N-bound chelate is 16 kcal.mol^{-1} higher in energy than the anionic O-bound chelate.

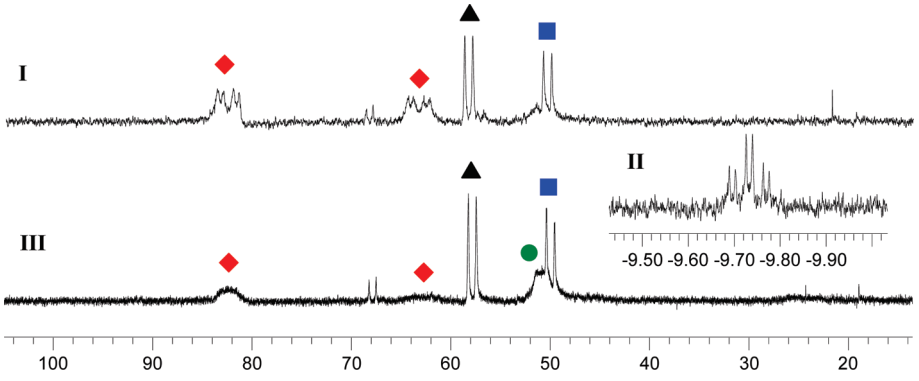

Figure 3. (I) High-pressure $^{31}P\{^{1}H\}$ NMR spectrum of [Rh(***H*L1**-κP)(**L1**-$\kappa^2 O,P$)(CO)] at 10 bar of CO/H_2. (II) ^{1}H NMR spectrum at 20 bar of CO/H_2. (III) $^{31}P\{^{1}H\}$ NMR spectrum at 20 bar of CO/H_2. Conditions: [Rh] = 40 mM, temp = 25 °C, solvent = CD_2Cl_2. The precursor complex [Rh(***H*L1**-κP)(**L1**-$\kappa^2 O,P$)(CO)] is represented by the red diamonds.

species that is formed under hydroformylation conditions.[15] An increase of the rhodium concentration from 1 to 15 mM led to an increase of the conversion from 6.2 to 33.2% (compare entries 1−4). However, when the rhodium concentration exceeds 5−10 mM, the conversion does not increase further presumably due to formation of inactive carbonyl-bridged dimeric rhodium species.[16] An increase of the partial CO pressure from 10 to 30 bar gave a decrease of the conversion from 26.5 to 18.7% (compare entries 2 and 6). Such a trend is normally observed in this reaction;[15] however, an increase in the partial H_2 pressure from 10 to 30 bar led to a remarkably strong increase of the conversion from 26.5 to 62.0% (compare entries 2 and 5). This result indicates that an increase of the partial H_2 pressure promotes the formation of the catalytically active hydride species from precursor complex [Rh(***H*L1**-κP)(**L1**-$\kappa^2 O,P$)(CO)], which is likely still present in the reaction mixture under these conditions.

Accordingly, we studied the anticipated precursor complex [Rh(***H*L1**-κP)(**L1**-$\kappa^2 O,P$)(CO)] under hydroformylation conditions via high-pressure NMR spectroscopy to observe the formation of the hydride species. The $^{31}P\{^{1}H\}$ NMR spectrum of the precursor complex in CD_2Cl_2 under a pressure of syngas (10 bar) shows that the precursor complex giving rise to the signals resonating at δ 63.0 and 81.9 ppm remains present in solution (Figure 3, I, red diamonds). The other major signals visible in the spectrum are a doublet resonating at δ 49.8 ppm (J_{Rh-P} = 163 Hz, blue squares), a broad signal resonating at δ 51 ppm (black triangle), and a doublet resonating at δ 58.1 ppm (J_{Rh-P} = 166 Hz, green circle) (Figure 3, I). One of these signals most likely belongs to the carbonyl-bridged dimeric rhodium species, as the NMR experiment is done at relatively high concentrations. In line with this, the color of the solution in the NMR tube turned to orange under syngas pressure, which is typical for this dirhodium species.[16] The ^{1}H NMR spectrum shows a single hydride signal (triplets of doublets) resonating at δ −9.74 ppm ($^{1}J_{H-Rh}$ = 6.7 Hz, $^{2}J_{H-P}$ = 18 Hz), which indicates that the hydride species is present in the solution carrying two equivalent ligands (Figure 3, II).[17] The relatively small H−P coupling constant reveals that the two ligands are predominantly coordinated in a bis-equatorial geometry.[18] The typical signals in the NMR spectra indicate that the identical coordinated ligands are both neutral. To convert precursor complex [Rh(***H*L1**-κP)(**L1**-$\kappa^2 O,P$)(CO)] into the hydride species, it reacts with a dihydrogen molecule to form a rhodium hydride and to transform the anionic chelating ligand into a neutral ligand. Increasing the pressure in the NMR tube to 20 bar of syngas decreased the amount of precursor complex in the solution in favor of the other species, which indicates that the composition of the reaction mixture is dependent on the pressure applied (Figure 3, III). These results are in accordance with studies by Trzeciak and Štěpnička on a related bis-ligated rhodium complex containing a neutral and an anionic *O*,*P*-chelating ligand.[8b] They found that with this type of complexes the hydride species is generated under hydroformylation conditions and also carries two neutral monodentate ligands.[8b] Depressurization of the solution in the NMR tube and changing to an atmosphere of argon regenerated the precursor complex [Rh(***H*L1**-κP)(**L1**-$\kappa^2 O,P$)(CO)] almost completely. These results imply that the precursor complex and the hydride species are in equilibrium, and the distribution of the species involved in this equilibrium is influenced by the pressure applied, in particular the partial pressure of H_2. Indeed, an increased hydroformylation activity of the precursor complex was observed by increasing the partial pressure of H_2, which is now well explained by the increase in the concentration of the active species (Table 1).

The NMR studies indicate a relatively fast establishment of the equilibrium between the hydride species and the precursor complex [Rh(***H*L1**-κP)(**L1**-$\kappa^2 O,P$)(CO)], which suggests that this complex is active in the hydroformylation reaction without a significant incubation time. To verify the absence of an incubation time, the hydroformylation of styrene using this complex was monitored via IR spectroscopy in combination with GC chromatography. Indeed, the kinetic profile shows immediate activity after pressurizing the reaction mixture with syngas, and there is no observable incubation time (Figure 4).[10] Furthermore, the positive order in alkene indicates that this system follows type I kinetics and that the observed positive order in H_2 in Table 1 is not related to type II kinetics, but merely to the equilibrium between the precursor complex and the hydride species.[15]

(15) Van Leeuwen, P. W. N. M.; Claver, C., Eds. *Rhodium Catalyzed Hydroformylation*; Kluwer Academic Publishers: Dordrecht, The Netherlands, 2000.

(16) Chan, A. S. C.; Shieh, H.-S.; Hill, J. R. *J. Chem. Soc., Chem. Commun.* **1983**, 688–689.

(17) Attempts to obtain the proton-coupled ^{31}P NMR spectrum in order to correlate couplings with the ^{1}H NMR spectrum failed, because of too large broadening of the peaks.

(18) Buisman, G. J. H.; van der Veen, L. A.; Kamer, P. C. J.; van Leeuwen, P. W. N. M. *Organometallics* **1997**, *16*, 5681–5687.

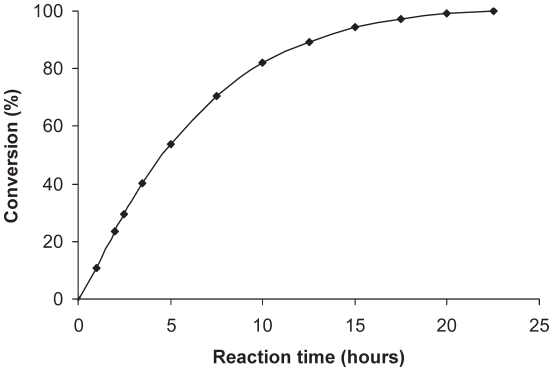

Figure 4. Kinetic profile of the hydroformylation of styrene using [Rh(*H*L1-κP)(L1-$\kappa^2 O,P$)(CO)]. Reaction conditions: [Rh] = 10 mM, Rh = [Rh(acac)$(CO)_2$], [*H*L] = 2.1 mM, [S] = 0.2 M, S = styrene, temp = 40 °C, pressure = 20 bar of 1:1 CO/H_2, solvent = CH_2Cl_2. The reaction was monitored *in situ* by way of the typical vibrations of the aldehyde product that arise in the IR spectrum with time. The intensity of the vibrations was calibrated by an independent determination of the conversion at the end of the reaction by means of GC (GC analysis after 23 h: conversion = 99%).

Although the equilibrium between the precursor complex and the hydride species is established, the position of this equilibrium in the catalytic cycle is still unclear. We considered therefore two conceivable pathways, for which we performed comparative DFT calculations starting from a model precursor complex **A**: [Rh(*H*L-κP)(L-$\kappa^2 O,P$)(CO)], L = 1,1-dimethyl-3-(diphenylphosphino)urea (Scheme 4). The initial steps in the catalytic cycle are identical in both pathways. Starting the catalytic cycle from the hydride species **B**, the acyl species **F** is formed via a series of steps involving the association of styrene to form **C**, migratory insertion of styrene to give **D**, association of CO to form **E**, and another migratory insertion step to form the acyl species **F**.[19] At this point, two different mechanisms are conceivable, which places the equilibrium between **A** and **B** within the hydroformylation cycle or as a equilibrium between a dormant state **A** and intermediate **B**.

Mechanism 1:. A pre-equilibrium mechanism. An intermolecular reaction involving the oxidative addition of H_2 dihydride to **F** leads to species **G***, which subsequently regenerates **B** via reductive elimination of the aldehyde. In this mechanism species **A** is in fact a dormant species in a pre-equilibrium *outside* the productive catalytic cycle.

Mechanism 2:. A ligand-assisted mechanism analogous to the reaction of phosphinourea ligands with [Rh(acac)$(CO)_2$] in Scheme 2, in which an acidic urea proton is transferred from a phosphinourea ligand in **F** to the acyl group via the metal center after an intramolecular acid−base reaction. In this pathway, an intramolecular oxidative addition of a phosphinourea ligand forms intermediate **G****, after which reductive elimination of the aldehyde regenerates species **A**. In this case the equilibrium between **A** and **B** is part of the catalytic cycle.

So far, we were unable to find a simple (nonsolvent assisted) intramolecular transition state to connect species **F** with **G****, because the urea proton from the phosphinourea in **F** points in the opposite direction from the urea oxygen (Figure 5). It thus seems that these static gas-phase DFT calculations, which disregard solvent-assisted (de)protonation, are of no further help to truly discriminate between these two possible mechanisms. Nonetheless, it is noteworthy that intermediate **G****, which occurs as a key intermediate in the ligand-assisted mechanism, lies 16.3 kcal mol^{-1} lower in energy than the intermediate **G***, which is the key intermediate in the pre-equilibrium mechanism. If a low-barrier (solvent assisted) route from **F** to **G** exists, the ligand-assisted mechanism is the preferred route for the reductive elimination of the aldehyde. In that case, the equilibrium between precursor complex **A** and hydride species **B** is integrated in the catalytic cycle and a new cooperative ligand-assisted mechanism of hydroformylation is operative.

We have demonstrated that the formation of [Rh(***H*L1***-κP)-(**L1**-$\kappa^2 O,P$)(CO)] involves a deprotonation of an acidic urea proton of one of the two phosphinourea ligands. Interestingly, this potentially allows the controlled formation of a heterobidentate ligand using two phosphinoureas having different acidity of the urea proton. For this reason, phosphoramidite phosphinourea ***H*L2** was prepared via a direct condensation reaction of *N*,*N*-dibenzylurea with a phosphorochloridite of (*S*)-2,2′-bisnaphthol in the presence of an excess of triethylamine base. This new ligand was fully characterized by ^1H, ^{13}C, and ^{31}P NMR and mass spectrometry.[10] By using equimolar equivalents of ***H*L1**, ***H*L2**, and [Rh(acac)$(CO)_2$] a metal complex was formed that shows in the $^{31}P\{^1H\}$ NMR spectrum two doublets of doublets (δ 63.3 and 170.9 ppm), indicating that a heteroligated complex has been formed with a *trans*-geometry of the two phosphorus donor atoms (Scheme 3, I). The $^{31}P\{^1H\}$ NMR spectrum of the new complex is very different from [Rh(***H*L1***-κP)(**L1**-$\kappa^2 O,P$)(CO)] (δ 62.9 and 82.0 ppm). In particular the downfield signal at 170.9 ppm, which belongs to ***H*L2**, indicates that this ligand forms the anionic chelate instead of ***H*L1** (Scheme 3, II). The ^1H NMR spectrum shows that acetylacetone (*H*acac) is displaced from the metal complex and that one urea proton is abstracted from ***H*L2**. Proton-coupled ^{31}P NMR and $^{31}P\{^1H\}-^1H$ 2D-NMR evidenced that the signal resonating at δ 63.3 ppm ($^1J_{P-Rh}$ = 131 Hz), corresponding to ***H*L1**, correlates to the urea proton still visible in the ^1H NMR spectrum. This result supports that the signal resonating at δ 170.9 ppm ($^1J_{P-Rh}$ = 190 Hz), corresponds to ***H*L2** as an anionic chelating ligand.[10] So, the ligand carrying the most acidic urea proton donates a proton to the $acac^-$ ligand in an acid−base reaction and forms the anionic chelate. This result confirms that by using two electronically different phosphinoureas a heteroligated complex is formed selectively. This provides a new tool in the area of combinatorial catalysis, as a large number of assembled catalysts can be prepared from a subset of well-chosen phosphinourea ligands.[20]

To demonstrate this new tool, we prepared rhodium complexes using six phosphinoureas (***H*L1**−***H*L6**) in a combinatorial

(19) Species outside the productive cycle are of minor importance to discriminate between the two pathways and are therefore not discussed here.

(20) For other examples of catalysts made in combinatorial fashion in rhodium-catalyzed hydroformylation see: (a) Goudriaan, P. E.; Kuil, M.; Jiang, X.-B.; van Leeuwen, P. W. N. M.; Reek, J. N. H. *Dalton Trans.* **2009**, 1801–1805. (b) Kuil, M.; Goudriaan, P. E.; Kleij, A. W.; Tooke, D. M.; Spek, A. L.; van Leeuwen, P. W. N. M.; Reek, J. N. H. *Dalton Trans.* **2007**, 2311–2320. (c) Slagt, V. F.; Röder, M.; Kamer, P. C. J.; van Leeuwen, P. W. N. M.; Reek, J. N. H. *J. Am. Chem. Soc.* **2004**, *126*, 4056–4057. (d) Kuil, M.; Goudriaan, P. E.; van Leeuwen, P. W. N. M.; Reek, J. N. H. *Chem. Commun.* **2006**, 4679–4681. (e) Slagt, V. F.; van Leeuwen, P. W. N. M.; Reek, J. N. H. *Chem. Commun.* **2003**, 2474–2475. (f) Slagt, V. F.; van Leeuwen, P. W. N. M.; Reek, J. N. H. *Angew. Chem., Int. Ed.* **2003**, *42*, 5619–5623. (g) Breit, B.; Seiche, W. *Angew. Chem., Int. Ed.* **2005**, *44*, 1640–1643. (h) Reetz, M. T.; Li, X. *Angew. Chem., Int. Ed.* **2005**, *44*, 2962–2964.

Scheme 3. (I) Reactivity of *H*L1 and *H*L2 with [Rh(acac)(CO)$_2$]; (II) ^{31}P{^{1}H} NMR Spectrum of the Resulting Complex [Rh(*H*L1-κP)(L2-$\kappa^2 O,P$)(CO)] (20 mM in $CDCl_3$)

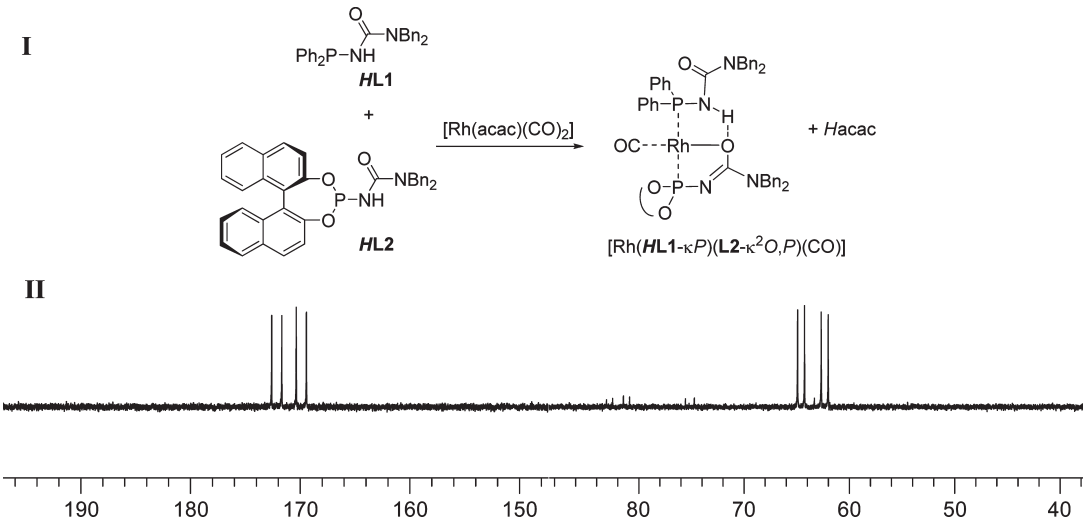

Scheme 4. DFT-Optimized Structures of the Two Mechanistic Pathways in the Hydroformylation of Styrene Using a Phosphinourea Metal Complex via Mechanism 1 (A *outside* the productive cycle) and Mechanism 2 (A *inside* the productive cycle)[a]

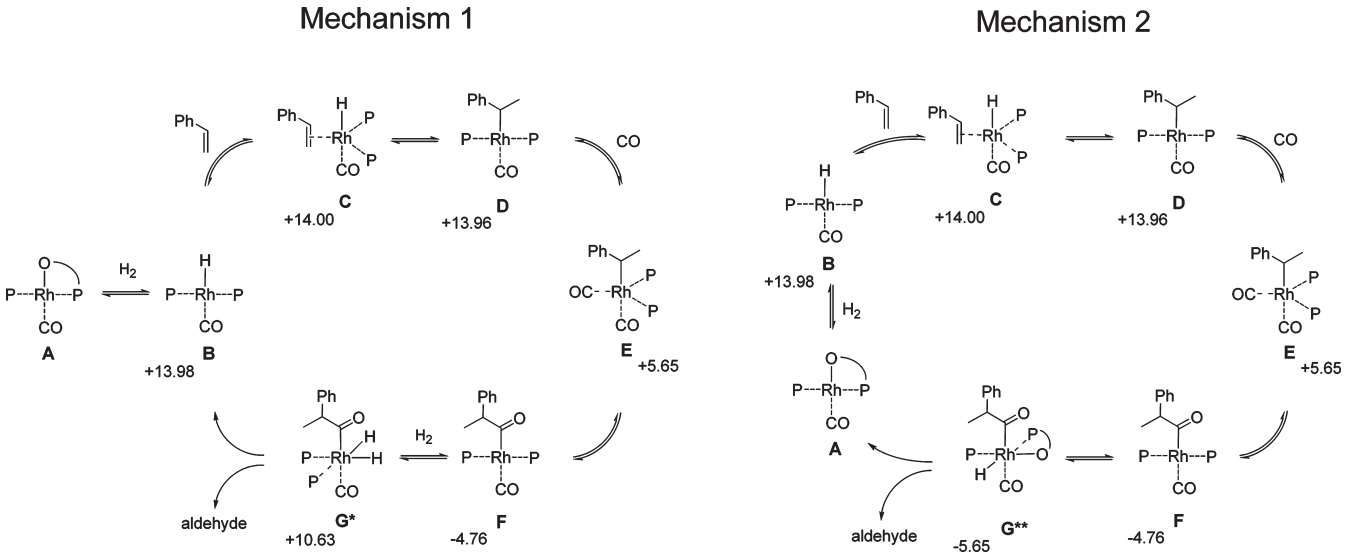

[a] Reported energies are relative to species **A** in kcal mol^{-1}. Nonproductive species have been omitted for clarity.

fashion, leading to 14 catalysts in total (6 homocombinations, 8 heterocombinations). These complexes were investigated in the asymmetric hydroformylation of styrene.[21] Besides ***H*L1**, all other ligands ***H*L2**−***H*L6** contain at least one chiral element in their ligand structure (Figure 6). ***H*L4** and ***H*L6** have a urea motif based on (*R*,*R*)-2,5-diphenylpyrrolidine, while ***H*L2**, ***H*L3**, and ***H*L5** contain a BINOL-based backbone. Ligand ***H*L6** contains both chiral elements.

The hydroformylation experiments were carried out at 40 °C in dichloromethane as a solvent at 20 bar of syngas pressure, and samples were analyzed after 18 h of reaction. Generally all catalysts gave good conversion (64.1−100%) and selectivity (85.7−96.6%) for the branched product (Table 2). The enantioselectivity displayed by the catalyst depends strongly on the ligands used (ee's between 0 and 46.4%). The homocombinations of the BINOL-based phosphoramidites ***H*L2**, ***H*L3**, ***H*L5**, and ***H*L6** all lead to poor selectivities, which suggest that this type of backbone is not an effective chiral element in the these complexes for the reaction studied. On the other hand, the homocombination of ***H*L4** was the most selective catalyst, providing an ee of 46.4%. Interestingly, this ligand contains the chirality on the urea motif only, which is remote from the metal center. Experiments in which the metal/ligand ratio was varied showed that the use of three equivalents of ***H*L4** gave practically the same ee of 45.9%, while using only one equivalent of ***H*L4** caused the ee to decrease to 38.2% (compare entries 4, 5, and 6). Ligand ***H*L6**, which contains a chiral center at the urea motif next to the BINOL backbone, gave poor selectivity (ee 6.8%). The heteroligated

(21) For selected examples for the asymmetric hydroformylation of styrene using traditional bidentate ligands see: (a) Sakai, N.; Mano, S.; Nozaki, K.; Takaya, H. *J. Am. Chem. Soc.* **1993**, *115*, 7033–7034. (b) Yan, Y.; Zhang, X. *J. Am. Chem. Soc.* **2006**, *128*, 7198–7202. (c) Robert, T.; Abiri, Z.; Wassenaar, J.; Sandee, A. J.; Romanski, S.; Neudörfl, J.-M.; Schmalz, H. G.; Reek, J. N. H. *Organometallics* **2010**, *29*, 478–483.

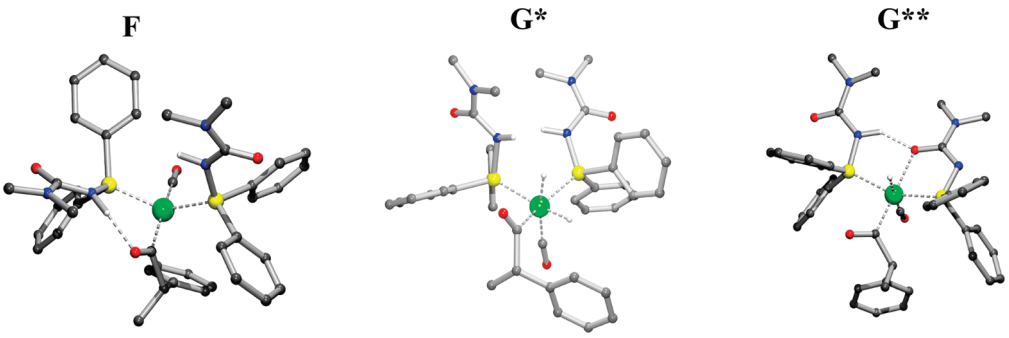

Figure 5. DFT (BP86, SV(P))-optimized structures of intermediates **F** (acyl species), **G***(oxidative addition of H_2), and **G**** (ligand-assisted intermediate). CH hydrogen atoms are omitted for clarity. Rh: green, P: yellow, O: red, N: blue, C: black, H: white.

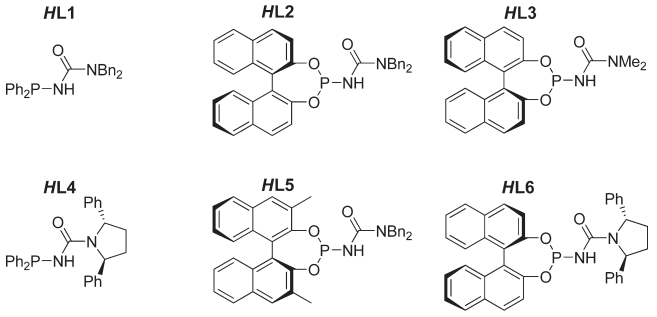

Figure 6. Structures of phosphinourea ligands ***H*L1**−***H*L6**.

Table 2. Asymmetric Hydroformylation of Styrene Using [Rh(*H*L-κ*P*)(L-κ^2*O*,*P*)(CO)]^a

entry	ligand	conversion (%)	branched (%)	ee (%)
1	***H*L1**	73.1	95.6	
2	***H*L2**	100	90.9	3.2 (*S*)
3	***H*L3**	80.6	85.7	0
4	***H*L4**	74.7	96.5	46.4 (*S*)
5^c	***H*L4**	99.1	96.6	38.2 (*S*)
6^d	***H*L4**	64.1	96.4	45.9 (*S*)
7	***H*L5**	100	93.9	3.4 (*R*)
8	***H*L6**	100	94.5	6.8 (*S*)
9	***H*L1** + ***H*L2**	96.7	93.8	4.5 (*S*)
10	***H*L1** + ***H*L3**	79.7	93.2	0
11	***H*L1** + ***H*L5**	100	94.3	2.7 (*S*)
12	***H*L1** + ***H*L6**	100	93.6	5.4 (*S*)
13^b	***H*L4** + ***H*L2**	91.8	94.2	24.5 (*S*)
14^b	***H*L4** + ***H*L3**	71.7	94.0	10.8 (*S*)
15^b	***H*L4** + ***H*L5**	98.3	95.1	25.0 (*S*)
16	***H*L4** + ***H*L6**	100	94.2	16.9 (*S*)

^{a} Reaction conditions: [Rh] = 10 mM, Rh = [Rh(acac)(CO)$_2$], [*H*L] = 21 mM, [S] = 1 M, S = styrene, reaction time = 18 h, temperature = 40 °C, pressure = 20 bar CO/H_2 (1:1), solvent = CH_2Cl_2. ^{b} Reaction time = 16 h. ^{c} [*H*L] = 10 mM. ^{d} [*H*L] = 30 mM.

complexes were prepared from phosphorus amides ***H*L1** and ***H*L4** in combination with the more acidic phosphoramidites ***H*L2**, ***H*L3**, ***H*L5**, and ***H*L6**. Unfortunately, these complexes did not yield more selective catalysts than the homocombinations in most examples. The most selective heterocombinations were ***H*L4** + ***H*L2** and ***H*L4** + ***H*L5**, giving ee's of 24.5 and 25.0%, respectively.

Conclusions

In summary, we report the synthesis of new phosphinourea ligands, the preparation of supramolecular homo- and heteroligated rhodium complexes thereof, and their use in the asymmetric hydroformylation of styrene. The hydroformylation reaction may well proceed via a new mechanism involving ligand cooperativity. This mechanism involves the reversible heterolytic splitting of H_2 over the metal center and an anionic phosphinourea fragment, and the ligand-assisted reductive elimination of the aldehyde. Computational studies support this ligand-assisted mechanism, but so far we cannot exclude a mechanism in which a dormant state and a rhodium hydride are in equilibrium via a reversible heterolytic splitting of H_2 over the metal center, connecting the dormant state with the productive hydroformylation cycle via a pre-equilibrium. The selective formation of heterobidentate ligands of these phosphinoureas is potentially a valuable strategy for the creation of catalyst libraries in a combinatorial fashion for high-throughput screening due to the straightforward ligand synthesis. The first results in this direction demonstrate that the application of a small ligand library already leads to catalysts that showed a high regioselectivity but so far moderate enantioselectivity. Surely, if larger libraries of this type are constructed, more selective catalysts will be uncovered.

Experimental Section

General Considerations. Unless stated otherwise, reactions were carried out under an inert atmosphere of nitrogen or argon using standard Schlenk techniques. THF was distilled from sodium benzophenone ketyl; CH_2Cl_2 was distilled from CaH_2, and toluene was distilled from sodium under nitrogen. Triethylamine was distilled from CaH_2 under nitrogen. With the exception of the compounds given below, all reagents were purchased from commercial suppliers and used without further purification. The following ligand precursor compounds were synthesized according to published procedures: phosphorochloridite of (*S*)- and (*R*)-2,2′-bisnaphthol,[22] phosphorochloridite of (*R*)-3,3′-dimethyl-2,2′-bisnaphthol,[23] and *N*,*N*-dibenzylurea.[24] NMR spectra were measured on a Varian Mercury (^{1}H: 300 MHz, ^{31}P{^{1}H}: 121.5 MHz, ^{13}C{^{1}H}: 75.5 MHz) or a Varian Inova spectrometer (^{1}H: 500 MHz, ^{31}P{^{1}H}: 202.3 MHz, ^{13}C{^{1}H}: 125.7 MHz) using dry solvents at room temperature unless stated otherwise. Chemical shifts are reported in ppm and are given relative to TMS (^{1}H and ^{13}C{^{1}H}) or H_3PO_4 (^{31}P{^{1}H}) as external standards. High-pressure NMR experiments were conducted using a glass NMR tube (New Era Enterprises, NE-HP5-M). 2D-NMR spectra were measured using a HMQC

(22) Buisman, G. J. H.; van der Veen, L. A.; Klootwijk, A.; de Lange, W. G. J.; Kamer, P. C. J.; van Leeuwen, P. W. N. M.; Vogt, D. *Organometallics* **1997**, *16*, 2929–2939.
(23) Huttenloch, O.; Laxman, E.; Waldmann, H. *Chem.—Eur. J.* **2002**, *8*, 4767–4780.
(24) Shi, F.; Smith, M. R.; Maleczka, R. E. *Org. Lett.* **2006**, 1411–1414.

pulse sequence without gradient. High-resolution mass spectra (HRMS) were recorded at the department of mass spectrometry at the University of Amsterdam using FAB^+ ionization on a JEOL JMS SX/SX102A four-sector mass spectrometer with 3-nitrobenzyl alcohol as the matrix. IR spectra were recorded on a Thermo Nicolet Nexus 670 FT-IR apparatus. High-pressure IR were carried out in a stainless steel 50 mL autoclave equipped with INTRAN windows (ZnS), a mechanical stirrer, a temperature controller, and a pressure indicator.

Synthesis of (2*R*,5*R*)-2,5-Diphenylpyrrolidine-1-carboxamide. (2*R*,5*R*)-2,5-Diphenylpyrrolidine (1.12 g, 1 equiv, 5 mmol) was placed in a round-bottom flask. Then 200 mL of distilled water was added, and the resulting suspension was vigorously stirred. A 2.75 mL portion of a 2 M aqueous HCl solution (5.5 mmol, 1.1 equiv) was added dropwise to the reaction mixture. After stirring for 1 h the reaction mixture turned clear and a solution of 7.5 mmol of KOCN (0.61 g, 1.5 equiv) in distilled water was added. The reaction mixture was next stirred for 48 h while the product precipitated from the reaction mixture. The product was filtered from the turbid reaction mixture and washed 3× with water and 3× with hexanes. Yield: 0.93 g (70%) as a white powder. ^{1}H NMR (300 MHz, $CDCl_3$): δ 1.74 (d, 2H, CH_2, J = 6.3 Hz), 2.48 (br, 2H, CH_2), 4.31 (s, 2H, NH_2), 5.04 (br, 1H, CH), 5.46 (br, 1H, CH), 7.2−7.5 (ArH, 10H). ^{13}C{^{1}H} NMR (75.5 MHz, $CDCl_3$): δ 31.342, 33.380, 62.157, 125.422, 125.923, 126.910, 128.107, 128.657, 129.336, 142.390, 143.846, 157.288 ($NH_2\underline{C}ON$). HRMS (FAB^+): m/z calcd for $C_{17}H_{19}N_2O$ ($[\overline{MH}]^+$) 267.1497, obsd 267.1501.

General Procedure for Phosphinourea Synthesis (phosphorus amide). *N*,*N*-Disubstituted urea (2 mmol, 1 equiv) was dried via coevaporation with toluene (3×) and dissolved in 40 mL of THF. After that the vigorously stirred reaction mixture was cooled to 0 °C, and 2.2 mmol (1.1 equiv) of *n*-BuLi was added dropwise. After 10 min 2 mmol of Ph_2PCl (1 equiv) was added dropwise to the vigorously stirred reaction mixture. The reaction mixture was allowed to heat to room temperature and stirred for 1 h. The reaction mixture was filtered over basic alumina, which washed with 2 × 10 mL of THF. The solvents from the collected filtrate were evaporated *in vacuo*. The product was redissolved in 20 mL of CH_2Cl_2 and filtered over a silica plug. The solvents of the collected filtrate were evaporated *in vacuo* to obtain the product.

***H*L1 (1,1-dibenzyl-3-(diphenylphosphino)urea).** Yield: 47%, white powder. ^{1}H NMR ($CDCl_3$, 500 MHz): δ 4.58 (s, 4H, CH_2), 5.04 (d, 1H, NH, $^2J_{H-P}$ = 6.9 Hz), 7.0−7.6 (m, 20H, ArH). ^{31}P{^{1}H} NMR ($CDCl_3$, 202.3 MHz): δ 25.518. ^{31}P NMR (CD_2Cl_2, 202.3 MHz): δ 25.518 (d, $^2J_{P-H}$ = 6.7 Hz). ^{13}C{^{1}H} NMR ($CDCl_3$, 125.7 MHz): δ 51.465 (CH_2), 127.498 (CH), 127.739 (CH), 128.528 (CH), 128.579 (CH), 128.958 (CH), 129.207 (CH), 130.996 (CH), 131.171 (CH), 137.732 (C_{quat}), 139.713 (C_{quat}), 139.837 (C_{quat}), 158.264 (d, NH$\underline{C}$ON, $^2J_{C-P}$ = 15 Hz). HRMS (FAB^+): m/z calcd for $C_{27}H_{26}\overline{N}_2OP$ ($[MH]^+$) 425.1783, obsd 425.1790. Solution IR (10 mM, $CDCl_3$): ν = 3412 cm^{-1} (NH band), 1650 cm^{-1} (CO band).

***H*L4 ((2*R*,5*R*)-*N*-(diphenylphosphino)-2,5-diphenylpyrrolidine-1-carboxamide).** Yield: 75%, white powder. ^{1}H NMR (300 MHz, CD_2Cl_2): δ 1.81 (d, 2H, CH_2, J = 5.7 Hz), 2.56 (s, 2H, CH_2), 4.82 (d, 1H, NH, $^2J_{H-P}$ = 7.5 Hz), 5.10 (br, 1H, CH), 5.56 (br, 1H, CH), 6.7−7.5 (ArH, 20H). ^{31}P{^{1}H} NMR (125.7 MHz, CD_2Cl_2): δ 23.53. ^{13}C{^{1}H} NMR (75.5 MHz, CD_2Cl_2): δ 31.289, 33.400, 62.417, 125.381, 126.036, 126.733, 128.249, 128.331, 128.493, 128.584, 128.620, 129.302, 130.126, 130.406, 131.203, 131.499, 139.716, 139.785, 139.902, 140.007, 142.891, 144.204, 155.569 (d, NH$\underline{C}$ON, $^2J_{C-P}$ = 18 Hz). HRMS (FAB^+): m/z calcd for $C_{29}\overline{H}_{28}N_2OP$ ($[MH]^+$) 451.1939, obsd 451.1935.

General Procedure for Phosphinourea Synthesis (phosphoramidite). *N*,*N*-Disubstituted urea (2 mmol, 1 equiv) was dried via coevaporation with toluene (3×), dissolved in 40 mL of THF, and cooled to 0 °C, and an excess of dry triethylamine was added. After 10 min 2 mmol of phosphorchloridite (1 equiv) dissolved in 10 mL of THF was added dropwise to the reaction mixture, which was stirred for 12 h. The product mixture was filtered over a basic alumina plug. Solvents were evaporated *in vacuo*. The product was redissolved in CH_2Cl_2 and filtered over a silica plug. The solvents were evaporated *in vacuo* to obtain the product. The ligands ***H*L2**, ***H*L3**, ***H*L5**, and ***H*L6** were obtained in a yield of 20−30% after filtration over silica.

***H*L2 ((*S*)-1,1-dibenzyl-3-(dinaphtho[2,1-*d*:1′,2′-*f*][1,3,2]dioxaphosphepin-4-yl)urea).** White powder. ^{1}H NMR (CD_2Cl_2, 500 MHz): δ 4.325 (br d, 2H, CH_2), 4.553 (br s, 2H, CH_2), 5.687 (d, 1H, NH, $^2J_{H-P}$ = 6.5 Hz), 7.1−7.6 (m, 18H, ArH), 7.8−8.1 (m, 4H, ArH). ^{31}P{^{1}H} NMR (CD_2Cl_2, 121.5 MHz): δ 144.459. ^{31}P NMR (CD_2Cl_2, 121.5 MHz): δ 144.459 (d, $^2J_{P-H}$ = 6.0 Hz). ^{13}C{^{1}H} NMR (CD_2Cl_2, 125.7 MHz): δ 50.300 (CH_2), 121.420 (CH), 121.759 (CH), 123.606 (C_{quat}), 124.257 (C_{quat}), 124.301 (C_{quat}), 125.117 (CH), 125.271 (CH), 125.322 (CH), 126.366 (CH), 126.480 (CH), 126.608 (CH), 126.715 (CH), 127.330 (CH), 127.689 (CH), 128.246 (CH), 128.478 (CH), 128.518 (CH), 128.820 (CH), 129.056 (CH), 130.076 (CH), 130.718 (CH), 131.319 (C_{quat}), 131.762 (C_{quat}), 132.668 (C_{quat}), 132.762 (C_{quat}), 146.845 (C_{quat}), 146.875 (C_{quat}), 148.500 (C_{quat}), 157.185 (d, NH$\underline{C}$ON, $^2J_{C-P}$ = 15 Hz). HRMS (FAB^+): m/z calcd for $C_{35}\overline{H}_{28}O_3N_2P$ ($[MH]^+$) 555.1838, obsd 555.1832. Solution IR (10 mM, $CDCl_3$): ν = 3408 cm^{-1} (NH_{free} band), 1646 cm^{-1} (CO_{urea} band).

***H*L3 ((*R*)-3-(dinaphtho[2,1-*d*:1′,2′-*f*][1,3,2]dioxaphosphepin-4-yl)-1,1-dimethylurea).** White powder. ^{1}H NMR ($CDCl_3$, 500 MHz): δ 2.86 (s, 6H, CH_3), 5.56 (d, 1H, NH, $^2J_{H-P}$ = 6.0 Hz), 7.2−7.6 (m, 8H, ArH), 7.9−8.1 (m, 4H, ArH). ^{31}P{^{1}H} NMR ($CDCl_3$, 202.3 MHz): δ 144.298. ^{13}C{^{1}H} NMR ($CDCl_3$, 125.7 MHz): δ 36.424 (CH_3), 121.542 (CH), 122.121 (CH), 123.933 (C_{quat}), 123.950 (C_{quat}), 124.323 (C_{quat}), 124.365 (C_{quat}), 125.151 (CH), 125.266 (CH), 126.441 (CH), 126.483 (CH), 126.908 (CH), 126.976 (CH), 128.317 (CH), 128.490 (CH), 128.515 (CH), 128.127 (CH), 129.852 (CH), 130.750 (CH), 131.302 (C_{quat}), 131.739 (C_{quat}), 132.820 (C_{quat}), 147.022 (C_{quat}), 147.054 (C_{quat}), 148.605 (C_{quat}), 156.906 (d, NH$\underline{C}$ON, $^2J_{C-P}$ = 15 Hz). HRMS (FAB^+): m/z calcd for $C_{23}H_{20}\overline{N}_2O_3P$ ($[MH]^+$) 403.1212, obsd 403.1216.

***H*L5 ((*R*)-1,1-dibenzyl-3-(2,6-dimethyldinaphtho[2,1-*d*:1′,2′-*f*]-[1,3,2]dioxaphosphepin-4-yl)urea).** White powder. ^{1}H NMR (CD_2Cl_2, 500 MHz): δ 2.48 (s, 3H, CH_3), 2.58 (s, 3H, CH_3), 4.3 (br, 2H, CH_2), 4.5 (br, 2H, CH_2), 5.72 (d, 1H, NH, $^2J_{H-P}$ = 6.9 Hz), 7.1−7.9 (m, 20H, ArH). ^{31}P{^{1}H} NMR (CD_2Cl_2, 202.3 MHz): δ 143.787. ^{13}C NMR (CD_2Cl_2, 75.5 MHz): δ 17.178, 17.422, 50.336, 123.418, 123.450, 124.297, 124.371, 124.961, 125.143, 125.249, 125.379, 126.480, 126.508, 127.407 (br), 127.593, 127.693, 128.765, 129.687, 130.075, 130.169, 130.190, 130.347, 131.110, 131.354, 131.373, 131.479, 11.500, 131.554, 136.708 (br), 146.218, 146.271, 147.520, 147.543, 157.206 (d, NH$\underline{C}$ON, $^2J_{C-P}$ = 16 Hz). HRMS (FAB^+): m/z calcd for $C_{37}H_{32}\overline{O}_3N_2P$ ($[MH]^+$) 583.2151, obsd 583.2154.

***H*L6 ((2*S*,5*S*)-*N*-((11b*R*)-dinaphtho[2,1-*d*:1′,2′-*f*][1,3,2]dioxaphosphepin-4-yl)-2,5-diphenylpyrrolidine-1-carboxamide).** White powder. ^{1}H NMR (CD_2Cl_2, 500 MHz): δ 1.77 (s, 2H, CH_2), 2.48 (br, 2H, CH_3), 4.78 (s, 1H, CH), 5.25 (d, 1H, NH, $^2J_{H-P}$ = 5.5 Hz), 5.56 (s, 1H, CH), 7.0−7.6 (m, 18H, ArH), 7.8−8.2 (m, 4H, ArH). ^{31}P{^{1}H} NMR (CD_2Cl_2, 202.3 MHz): δ 145.497. ^{13}C{^{1}H} NMR (CD_2Cl_2, 75.5 MHz): δ 31.015 (CH_2), 33.410 (CH_2), 62.056 (CH), 121.446 (CH), 122.121 (CH), 123.872 (C_{quat}), 123.974 (C_{quat}), 124.016 (C_{quat}), 124.994 (CH), 125.043 (CH), 125.357 (CH), 126.229 (CH), 126.767 (CH), 126.904 (CH), 127.734 (CH), 128.314 (CH), 128.515 (CH), 128.871 (CH), 129.417 (CH), 130.410 (CH), 131.213 (C_{quat}), 131.478 (C_{quat}), 132.634 (C_{quat}), 132.737 (C_{quat}), 141.253 (C_{quat}), 143.421 (C_{quat}), 146.912 (C_{quat}), 146.942 (C_{quat}), 148.428 (C_{quat}), 154.932 (d, NH$\underline{C}$ON, $^2J_{C-P}$ = 15 Hz). HRMS (FAB^+): m/z calcd for $C_{37}H_{30}\overline{O}_3N_2P$ ($[MH]^+$) 581.1994, obsd 581.1999.

General Procedure for Complex Synthesis. To a Schlenk filled with 1 mmol (2 equiv) of phosphinourea ligand and 0.5 mmol

(129 mg, 1 equiv) of [Rh(acac)(CO)$_2$] was added 10 mL of CH_2Cl_2. Instantaneously CO gas was released from the clear yellow reaction mixture. After five minutes of vigorous stirring, solvents were evaporated *in vacuo*. *H*acac (acetylacetone) present as a side-product was removed via coevaporation with toluene (3×). The complexes were formed in high purity (> 95% based on $^{31}P\{^1H\}$ NMR) and were used without further purification.

Complex [Rh(*H*L1-κP)(L1-$\kappa^2 O,P$)(CO)]. Yellow-orange powder. ^1H NMR (CD_2Cl_2, 500 MHz): δ 4.24 (s, 6H, CH_2), 4.81 (s, 2H, CH_2), 6.4 (d, 1H, NH, $^2J_{H-P} = 16.5$ Hz), 7.0−7.8 (m, 40H, ArH). $^{31}P\{^1H\}$ NMR (CD_2Cl_2, 202.3 MHz): δ 62.9 (dd, $^1J_{Rh-P} = 135$ Hz, $^2J_{P-P} = 326$ Hz), 82.0 (dd, $^1J_{Rh-P} = 129$ Hz, $^2J_{P-P} = 326$ Hz). ^{31}P NMR ($CDCl_3$, 202.3 MHz): δ 62.9 (dddt, $^1J_{Rh-P} = 135$ Hz, $^2J_{P-P} = 326$ Hz, $^2J_{P-H} = 14.6$ Hz, $^3J_{Ar-H} = 11.7$ Hz), 82.0 (ddt, $^1J_{Rh-P} = 129$ Hz, $^2J_{P-P} = 326$ Hz, $^3J_{Ar-H} = 11$ Hz). $^{13}C\{^1H\}$ NMR (CD_2Cl_2, 125.7 MHz): δ 49.605 (CH_2), 50.406 (CH_2), 126.877 (CH), 127.492 (CH), 127.573 (CH), 127.703 (CH), 127.796 (CH), 128.072 (CH), 128.158 (CH), 128.306 (CH), 128.391 (CH), 128.731 (CH), 129.846 (CH), 130.541 (CH), 131.301 (CH), 131.402 (CH), 132.934 (CH), 133.057 (CH), 133.625 (C_{quat}), 134.003 (C_{quat}), 136.948 (C_{quat}), 138.682 (C_{quat}), 138.755 (C_{quat}), 139.218 (C_{quat}), 155.424 (d, C_{quat}, $^2J_{C-P} = 7.4$ Hz, (NHCON), 175.5 (dd, C_{quat}, $^2J_{C-Rh} = 27$ Hz, $^2J_{C-P} = 8.8$ Hz, NCON), 192 (br d, C_{quat}, $^1J_{C-Rh} \approx 73$ Hz, Rh-CO). HRMS (FAB$^+$): *m*/*z* calcd for $C_{54}H_{49}N_4O_2P_2Rh$ ([MH]$^+$) 950.2386, obsd 950.2380 (CO ligand dissociated). Solution IR (10 mM, $CDCl_3$): $\nu = 3381$ cm^{-1} ($NH_{assoc.}$ band), 1970 cm^{-1} (Rh-CO band), 1663 cm^{-1} (CO_{urea} band).

Complex [Rh(*H*L2-κP)(L2-$\kappa^2 O,P$)(CO)]. Yellow-orange powder. ^1H NMR (CD_2Cl_2, 500 MHz): δ 4.2 (m, 4H, CH_2), 4.56 (s, 3H, CH_2), 5.88 (s, 1H, CH_2), 7.2−8.2 (m, 45H, ArH+NH). $^{31}P\{^1H\}$ NMR (CD_2Cl_2, 202.3 MHz): δ 149.4 (dd, $^1J_{Rh-P} = 213$ Hz, $^2J_{P-P} = 674$ Hz, 170.0 (dd, $^1J_{Rh-P} = 189$ Hz, $^2J_{P-P} = 672$ Hz). HRMS (FAB$^+$): *m*/*z* calcd for $C_{70}H_{54}N_4O_6P_2Rh$ ([MH]$^+$) 1211.2574, obsd 1211.2566 (CO ligand dissociated).

Complex [Rh(*H*L1-κP)(L2-$\kappa^2 O,P$)(CO)]. Yellow-orange powder. ^1H NMR (CD_2Cl_2, 500 MHz): δ 3.76 (d, 1H, CH_2, $J = 15.5$ Hz), 4.07 (d, 1H, CH_2, $J = 15$ Hz), 4.2 (br, 4H, CH_2) 4.46 (d, 1H, CH_2, $J = 15$ Hz), 4.95 (d, 1H, CH_2, $J = 15.5$ Hz), 6.33 (d, 1H, NH, $^2J_{H-P} = 17$ Hz) 6.8−8.0 (m, 42H, ArH). $^{31}P\{^1H\}$ NMR (CD_2Cl_2, 202.3 MHz): δ 63.3 (dd, $^1J_{Rh-P} = 131$ Hz, $^2J_{P-P} = 451$ Hz), 170.9 (dd, $^1J_{Rh-P} = 190$ Hz, $^2J_{P-P} = 451$ Hz). ^{31}P NMR (CD_2Cl_2, 202.3 MHz): δ 63.3 (dddt, $^1J_{Rh-P} = 131$ Hz, $^2J_{P-P} = 451$ Hz, $^2J_{P-H} = 13.8$ Hz, $^3J_{Ar-H} = 12.5$ Hz) 170.9 (dd, $^1J_{Rh-P} = 190$ Hz, $^2J_{P-P} = 451$ Hz). HRMS (FAB$^+$): *m*/*z* calcd for $C_{62}H_{52}O_4N_4P_2Rh$ ([MH]$^+$) 1081.2519, obsd 1081.2521 (CO ligand dissociated).

General Procedure for Hydroformylation Experiments. The hydroformylation experiments were carried out in a stainless steel autoclave (volume 150 mL) with an insert for five 2 mL glass reaction vials. The reaction vials were dried in an oven (135 °C), capped with a septum, and flushed with inert gas (argon) before use. In each reaction vial the catalyst was made *in situ* by charging the reaction vial with the appropriate amounts of metal precursor and ligands before it was flushed again with inert gas. The substrate (styrene) was filtered freshly over basic alumina to remove peroxide impurities. The substrate was dissolved in CH_2Cl_2 at the appropriate molarity and was injected into the reaction vials. The insert containing the reaction vials was placed in the autoclave, which was closed thoroughly. Before starting the catalytic reaction, the prepared autoclave was purged three times with 10 bar of syngas (CO/H_2 = 1:1) and then pressurized to the appropriate pressure. The pressure in the autoclave during the reaction was monitored by either an analog or digital readout. The reaction was stopped by cooling the autoclave with ice, and the autoclave was subsequently slowly depressurized. Reaction samples were prepared and analyzed directly after the reaction by GC chromatography using an Interscience Focus GC equipped with a Supelco beta dex 225 column.

X-ray Crystallography of *H*L1. $C_{27}H_{25}N_2OP$, $M_w = 424.46$, colorless rod, 0.32 × 0.14 × 0.10 mm^3, triclinic, $P\bar{1}$ (No. 2), $a = 9.3963(4)$ Å, $b = 10.0852(4)$ Å, $c = 20.8958(12)$ Å, $\alpha = 92.021(2)°$, $\beta = 100.289(2)°$, $\gamma = 108.447(2)°$, $V = 2203.99(18)$ Å^3, $Z = 4$, $D_{exptl} = 1.279$ g/cm^3, μ(Mo Kα) = 0.147 mm^{-1}, $T = 110$ K. X-ray data were collected (θ(max) = 27.5°; total = 57 422; unique = 10124) on a Nonius KappaCCD with graphite-monochromated Mo Kα radiation ($\lambda = 0.71073$ Å) under program control of COLLECT.[25] The program PEAKREF[26] was used to determine the cell dimensions. Data reduction was done using the program EVALCCD.[27] Absorption correction based on face-indexing was done with SADABS.[28] The structure was solved with SHELXS-97[29] and refined with SHELXL-97.[29] Hydrogen atoms were introduced at calculated positions and refined riding on their carrier atoms with U(iso) = 1.2 × U_{eq} of the attached C atom. The H atoms attached to N2A and N2B were located from a difference map and refined with a distance restraint [d(N−H) − 0.88 Å]. Final $R = 0.0415$ for 7278 reflections with $I > 2\sigma(I)$, $wR_2 = 0.0948$ for 10 124 reflections, $S = 1.02$, $N_{param} = 565$. The final difference map is essentially featureless with excursions in the range −0.36 to 0.43 e/Å^3. The structure was validated with PLATON/CHECK.[30] The cif file of **L1** is supplied in the Supporting Information.

DFT Calculations. The geometry optimizations were carried out with the Turbomole program[31] coupled to the PQS Baker optimizer.[32] All geometries were optimized at the BP86[33] level using the SV(P) basis set[34] on all atoms (small-core pseudopotential[35] on rhodium). Optimized geometries of the species are supplied as a pdf file in the Supporting Information.

Acknowledgment. This research is financially supported by BASF The Netherlands and the Dutch Ministry of Economic Affairs by way of SenterNovem. J. W. H. Peeters is acknowledged for the mass spectrometry experiments, J. M. Ernsting for assistance with the 2D-NMR experiments, and Z. Abiri for providing *N*,*N*-dibenzylurea.

Supporting Information Available: This material is available free of charge via the Internet at http://pubs.acs.org.

(25) *COLLECT*; Nonius BV: Delft, The Netherlands, 1999.
(26) Schreurs, A. M. M. *PEAKREF*; Utrecht University: Utrecht, The Netherlands, 2005.
(27) Duisenberg, A. J. M.; Kroon-Batenburg, L. M. J.; Schreurs, A. M. M. *J. Appl. Crystallogr.* **2003**, *36*, 220–229.
(28) Sheldrick, G. M. *SADABS 2006/1*; University of Göttingen: Göttingen, Germany, 2006.
(29) Sheldrick, G. M. *Acta Crystallogr., Sect. A* **2008**, *64*, 112–122.
(30) Spek, A. L. *Acta Crystallogr. Sect. D* **2009**, *65*, 148–155.
(31) (a) Ahlrichs, R.; Bär, M.; Baron, H.-P.; Bauernschmitt, R.; Böcker, S.; Ehrig, M.; Eichkorn, K.; Elliott, S.; Furche, F.; Haase, F.; Häser, M.; Hättig, C.; Horn, H.; Huber, C.; Huniar, U.; Kattannek, M.; Köhn, A.; Kölmel, C.; Kollwitz, M.; May, K.; Ochsenfeld, C.; Öhm, H.; Schäfer, A.; Schneider, U.; Treutler, O.; Tsereteli, K.; Unterreiner, B.; von Arnim, M.; Weigend, F.; Weis, P.; Weiss, H. *Turbomole Version 5*; Theoretical Chemistry Group, University of Karlsruhe, **2002**. (b) Treutler, O.; Ahlrichs, R. *J. Chem. Phys.* **1995**, *102*, 346–354.
(32) (a) *PQS* version 2.4; Parallel Quantum Solutions: Fayetteville, AR, 2001 (the Baker optimizer is available separately from PQS upon request). (b) Baker, J. *J. Comput. Chem.* **1986**, *7*, 385–395.
(33) (a) Becke, A. D. *Phys. Rev. A* **1988**, *38*, 3098–3100. (b) Perdew, J. P. *Phys. Rev. B* **1986**, *33*, 8822–8824.
(34) Schäfer, A.; Horn, H.; Ahlrichs, R. *J. Chem. Phys.* **1992**, *97*, 2571–2577.
(35) (a) Turbomole basis set library, *Turbomole* Version 5. (b) Andrae, D.; Haeussermann, U.; Dolg, M.; Stoll, H.; Preuss, H. *Theor. Chim. Acta* **1990**, *77*, 123–141.